research article

Bladder paraganglioma: CT and MR imaging characteristics in 16 patients

Jing Zhang[1], Xu Bai[2], Jing Yuan[3], Xiaojing Zhang[1], Wei Xu[1], Huiyi Ye[1], Haiyi Wang[1]

[1] Department of Radiology, First Medical Center, Chinese PLA General Hospital, Beijing, China
[2] Department of Radiology, Fifth Medical Center, Chinese PLA General Hospital, Beijing, China
[3] Department of Pathology, Tianjin Nankai Hospital, Tianjin, China

Radiol Oncol 2022; 56(1): 46-53.

Received 3 August 2021
Accepted 24 November 2021

Correspondence to: Haiyi Wang M.D., Department of Radiology, First Medical Centre, Chinese PLA General Hospital, No. 28 Fuxing Road, Haidian District, Beijing 100853, China. E-mail: wanghaiyi301@outlook.com

Jing Zhang and Xu Bai contributed equally.

Disclosure: No potential conflicts of interest were disclosed.

Background. Bladder paraganglioma (BPG) is a rare extra-adrenal pheochromocytoma with variable symptoms and easy to be misdiagnosed and mishandled. The aim of the study was to document the imaging features of BPG using computed tomography (CT) and magnetic resonance imaging (MRI).

Patients and methods. We retrospectively enrolled consecutive patients with pathology-proven BPG, who underwent CT or MRI examinations before surgery between October 2009 and October 2017. The clinical characteristics, CT, and MRI features of the patients were described and analysed.

Results. A total of 16 patients with 16 bladder tumours (median age 51 years, 9 females) were included. Among them, 13 patients underwent CT examinations and eight patients underwent MRI examinations preoperatively. Tumour diameters ranged from 1.6−5.4 cm. Most of the tumours grew into the bladder cavity (n = 11) with oval shapes (n = 10) and well-defined margins (n = 14). Intratumour cystic degeneration or necrosis (n = 2) was observed. Two lesions showed peripheral tissue invasion, suggesting malignant BPGs. All 13 lesions imaged with CT exhibited slight hypoattenuation and moderate to marked enhancement. Compared to the *gluteus maximus*, all lesions showed slight hyperintensity in T2-weighted images, hyperintensity on diffusion-weighted images (DWI), hypointensity on apparent diffusion coefficient maps, hyperintensity on T1-weighted images and a "fast in and slow out" enhanced pattern on contrast-enhanced MRI images.

Conclusions. BPGs are mostly oval-shaped, broadly-based and hypervascular bladder tumours with hypoattenuation on non-contrast CT, T2 hyperintensity, slight T1 hyperintensity compared to the muscle, marked restricted diffusion on DWI. Peripheral tissue invasion can suggest malignancy of the BPGs. All of these features contribute to preoperative decision-making.

Key words: paraganglioma; urinary bladder; computed tomography; magnetic resonance imaging

Introduction

Paragangliomas are rare neoplasms of extra-adrenal chromaffin cells that belong to the family of neuroendocrine tumours.[1] They account for 15–20% of pheochromocytomas and occur in a variety of locations such as the head and neck, paraspinal region, chest, abdomen, and pelvis. The bladder is the most common site of paragangliomas in the genitourinary system (79.2%).[2]

Bladder paragangliomas (BPGs) are exceedingly rare and constitute only 0.06% of bladder tumours and 1% of all paragangliomas.[3] BPG is an extra-adrenal pheochromocytoma that arises from the chromaffin tissue of the sympathetic nervous system associated with the bladder wall and has

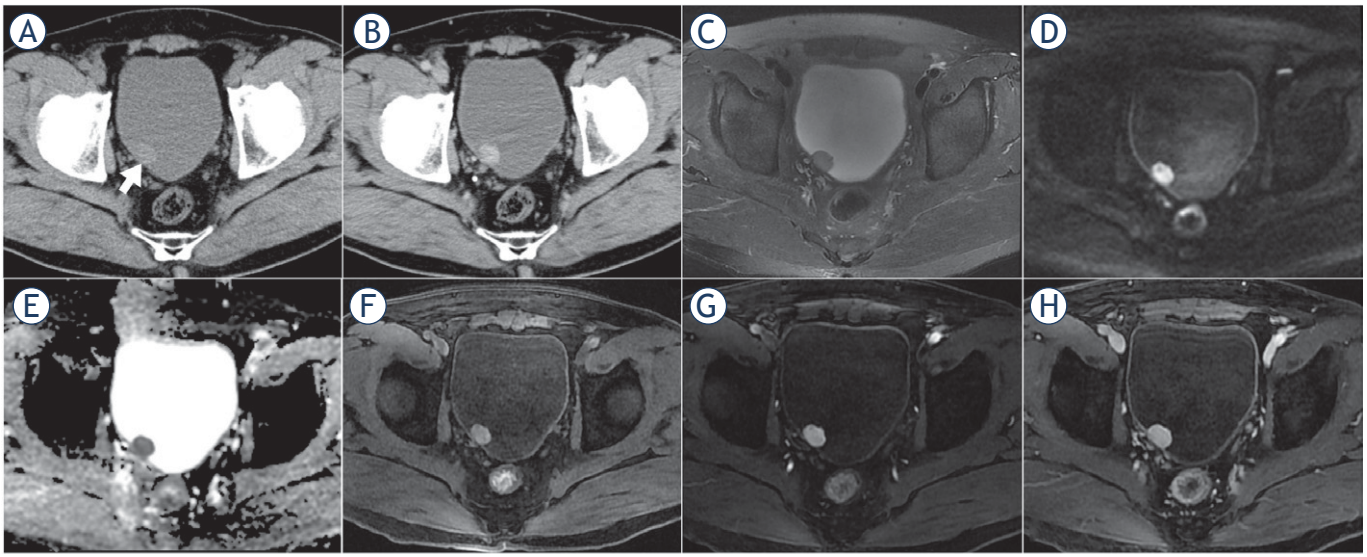

FIGURE 1. CT and MR images of a 61-year-old male patient with bladder paraganglioma. The tumour was located in the posterior bladder wall, oval, well-defined margin, protruding into the bladder cavity with broad-base attachment to the bladder wall (short arrow). The lesion showed slight hypodensity and obvious enhancement on axial pre- and post-contrast-enhanced CT images **(A, B)**, homogenous slight hyperintensity on T2-weighted images (T2WI) **(C)**, marked hyperintensity on diffusion-weighted images (DWI) **(D)**, hypointensity on apparent diffusion coefficient (ADC) maps (mean ADC value, 0.870 × 10^{-3} mm^2/s) **(E)**, hyperintensity compared to the *gluteus maximus* on T1-weighted images (T1WI) **(F)** and "fast in and slow out" on dynamic contrast-enhanced MRI **(G, H)**.

the potential to secrete catecholamines (norepinephrine, epinephrine, and dopamine).[2] The surgical preparation and procedure therefore needs to be effectively formulated to avoid life-threatening malignant cardiovascular events caused by a burst release of catecholamines.[4] Due to its rarity and symptomatic variability[5], the disorder can easily be misdiagnosed and mishandled. Thus, accurate preoperative diagnosis is crucial.

In the present study, a series of 16 patients with BPG treated in our institution over an eight-year period were retrospectively reviewed and the computed tomography (CT) and magnetic resonance imaging (MRI) characteristics of BPG were analysed.

Patients and methods

The study was conducted in accordance with the Declaration of Helsinki and was approved by the Institutional Review Board of The First Medical Center of Chinese PLA General Hospital. Written informed consent was obtained from all patients. A computerized search of the hospital's pathology databases for BPGs from October 2009 to October 2017 was performed. During this period, there were 29 adult patients (age > 18 years) with 29 pathology-proven BPGs. This list of patients was then cross referenced with the institutional radiology database to identify the patients who underwent preoperative pelvic CT and/or MRI examinations. This yielded 16 patients with BPGs, which comprised our study population. Among them, 13 underwent contrast-enhanced CT examinations, eight underwent non-enhanced (n = 1) and dynamic contrast-enhanced (n = 7) MRI examinations, and five underwent both CT and MR preoperative examinations.

CT examinations were performed with GE Light Speed 16-row scanner (Milwaukee, WI, USA) (n = 3), Siemens Somatom 64-row scanner (Erlangen, Germany) (n = 5), Siemens Sensation Cardiac 64-row scanner (Erlangen, Germany) (n = 3) and GE Optima CT660 128-row spiral scanner (Milwaukee, WI, USA) (n = 2). All examinations were performed using similar scanning parameters with a slice thickness of 5 mm, 1.5 mm reconstruction, 120 kVp, and 500 mA. Nonionic contrast agents (Ultravist, Bayer HealthCare, Berlin, Germany; Iohexol, Beilu, Beijing, China) were used, dose 90–100 ml, injection rate 3.5 ml/s. Contrast-enhanced CT images were only acquired in the arterial phase (30~35s after contrast agent injection). The patients fasted for 4–6 h and were

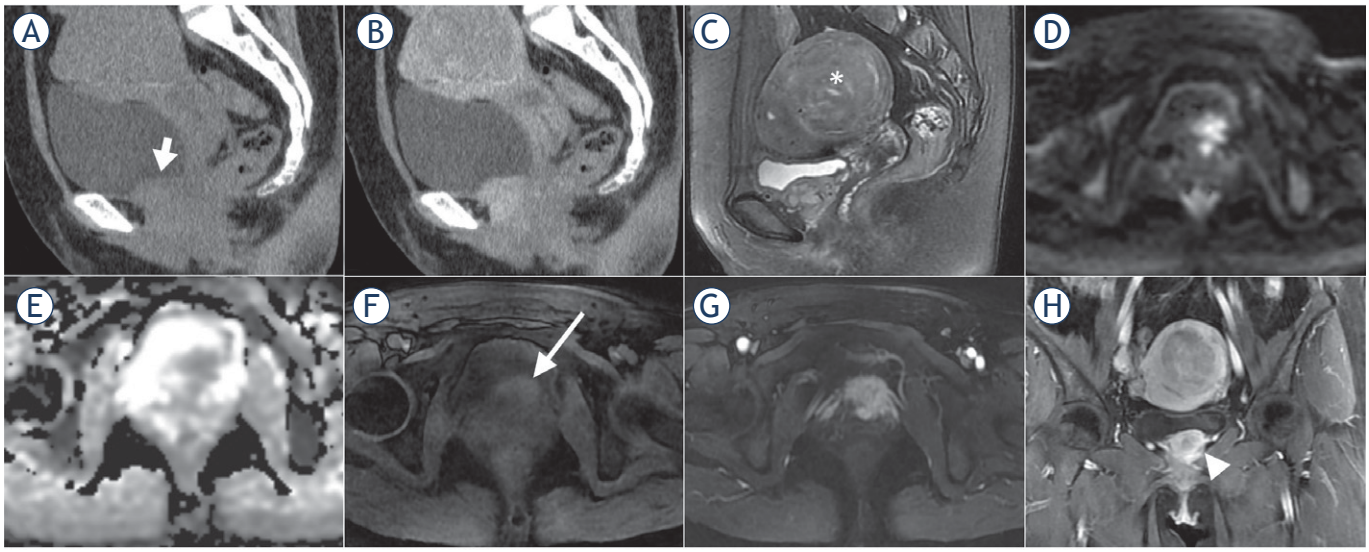

FIGURE 2. CT and MR images of a 47-year-old female with malignant bladder paraganglioma. The bladder tumour was located in the inferior bladder wall with an irregular shape and ill-defined margin, invading the adjacent tissues (short arrow). The tumour showed iso-density and moderate enhancement on sagittal pre- and post-contrast enhanced CT images **(A, B)**, inhomogenous hyperintensity on sagittal T2-weighted images (T2WI) **(C)**, hyperintensity on diffusion-weighted images (DWI) **(D)**, hypointensity on apparent diffusion coefficient (ADC) maps (mean ADC value, 0.852 × 10^{-3} mm^2/s) **(E)**, inhomogenous slight hyperintensity compared to the *gluteus maximus* on T1-weighted images (T1WI) (long arrow) **(F)**, heterogenous marked enhancement on arterial phase **(G)** and coronal contrast-enhanced images (arrowhead) **(H)**. In addition, a uterine fibroid on the posterior wall of the uterus was also found (asterisk on sagittal T2WI).

TABLE 1. Clinical characteristics of patients with bladder paraganglioma

Characteristics	Number (%) of patients
Median age in years (interquartile range)	51 (40, 63)
Sex	
Male	7 (43.8)
Female	9 (56.2)
Clinical manifestations	
Postmicturition syndrome*	6 (37.5)
Hypertension	3 (18.8)
Hematuria or progressive dysuria	3 (18.7)
24-h urinary VMA and CA level	
Not measured	11 (68.8)
Normal	4 (25.0)
Elevated	1 (6.2)
Tumor number	
Single	14 (87.5)
Multiple	2 (12.5)
Surgical approach	
Partial cystectomy	7 (43.8)
Local resection of bladder tumor**	9 (56.2)
Imaging methods	
Computerized tomography	13 (81.3)
Magnetic resonance imaging	8 (50.0)

CA = catecholamine; VMA = vanillylmandelic acid;

* postmicturition syndrome includes symptoms of catecholamine release such as sweating, palpitations, headaches, hypertension and syncope;
** local resections include transurethral laser and electric resection of bladder tumor

given water 30 min before the examination. The acquisition was performed with the bladder full of urine, from the inferior symphysis pubis to the apex of the bladder.

MRI examinations were performed with GE Signa Excite 1.5T and 3.0T MR imaging system (Milwaukee, WI, USA) (n = 5), and GE Signa HDxt 3.0T MR imaging system (Milwaukee, WI, USA) (n = 3). Patients were imaged in the supine position using an eight-channel surface phased-array coil. Pelvic MRI sequences and parameters were as follows: axial, sagittal and coronal fast spin echo (FSE) T2-weighted images (T2WI): repetition time (TR) / echo time (TE), infinite / 90–105 ms; field of view (FOV), 36×44cm; slice thickness / interlayer distance, 5.0 mm / 0.5 mm; and matrix, 320 × 224. Diffusion-weighted images (DWI) using single-shot echo planar imaging (SE-EPI): b values, 0 / 800 s/mm^2; TR / TE, 2500–5000 / 60–65 ms; FOV, 36×44 cm; slice thickness / interlayer distance, 5.0 mm / 0.5 mm; and matrix, 128×128. Axial gradient recalled echo (GRE) T1-weighted images (T1WI): TR / TE, 3.2–4.5 / 1.5–2.2 ms; FOV, 36×44 cm; slice thickness / interlayer distance, 5.0 mm / −2.5 mm; and matrix, 288 × 224. Dynamic contrast enhanced T1WI was performed in the axial plane during the arterial phase, venous phase, and delayed phase. Gadobenate dimeglumine (MultiHance; Bracco

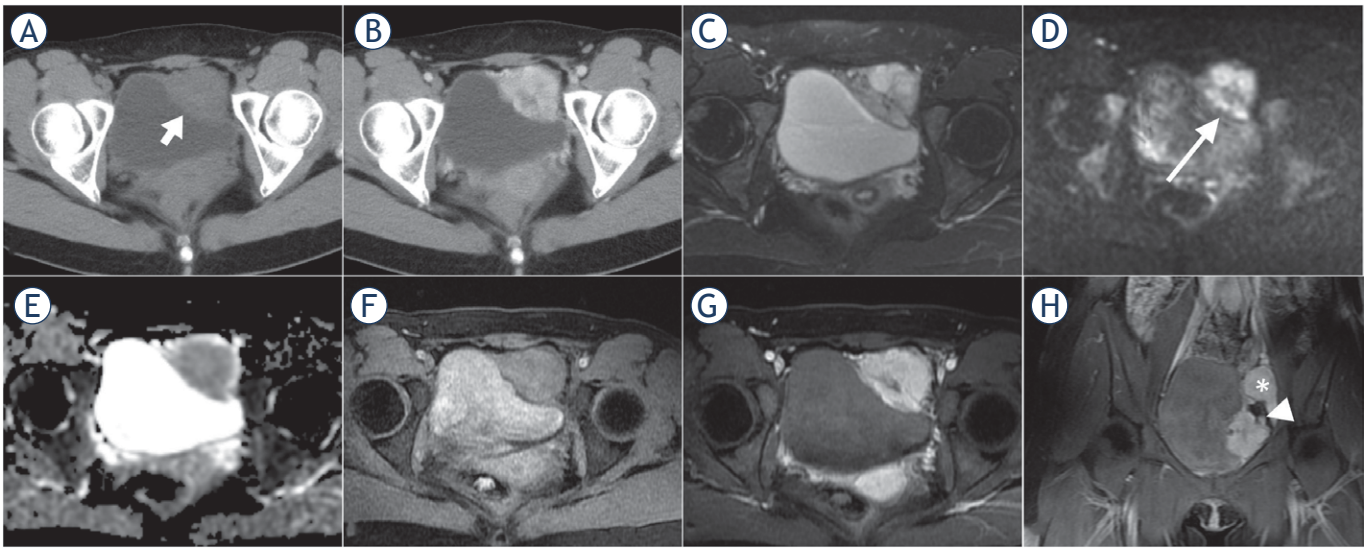

FIGURE 3. CT and MR images of a 25-year-old female with malignant bladder paraganglioma. The tumour was located in the left bladder wall with irregular shape, presenting heterogenous hypodensity (short arrow) and obvious enhancement on axial pre- and post-contrast enhanced CT images **(A, B)**, heterogenous slight or marked hyperintensity on T2-weighted images (T2WI) **(C)**, heterogenous hyperintensity on diffusion-weighted images (DWI) (long arrow) **(D)**, hypointensity on apparent diffusion coefficient (ADC) maps (mean ADC value, 0.997×10^{-3} mm^2/s) **(E)**, slight hyperintensity compared to the gluteus maximus on T1WI (**F**) and early marked enhancement on arterial phase images **(G)**. Coronal enhanced MRI showed the lesion encased the left iliac artery branch (arrowhead); a similar enhanced lesion was located next to the left iliac vessels (asterisk), suggesting multiple paraganglioma **(H)**.

Sine, Shanghai, China) was injected intravenously at a dosage of 0.1 mmol/kg as a rapid bolus injection at a rate of 2 mL/s with a power injector (Spectris Solaris EP, Medrad, Indianola, PA, USA), followed by a 20 mL saline flush.

Two experienced abdominal radiologists (Huiyi Ye and Haiyi Wang, with 30 and 20 years of experience, respectively) at our institution reviewed the CT or MR image characteristics of each lesion, and reached a consensus on imaging analysis. The imaging parameters observed included the location, size, shape, margin, density / signal intensity, enhancement pattern, cystic degeneration/necrosis, haemorrhage, and calcification. On pre- / post-contrast enhanced CT and MR images, the density and signal intensity relative to the *gluteus maximus* at the same layer were measured. The area of interest (ROI) was determined based on avoiding cystic degeneration and necrosis in the lesion. The mean apparent diffusion coefficient (ADC) value was measured by drawing a ROI over the most hypointense area within the tumour on the ADC maps

Blind to the image findings, all specimens were reviewed by an experienced uropathologist (Jing Yuan with 15 years of experience) according to the World Health Organization Classification of Tumours of Endocrine Organs.[6]

TABLE 2. Location and morphological characteristics of bladder paraganglioma

Characteristics	Number (%) of patients
Mean maximum diameter of tumour (cm)*	2.6 ± 1.0
Location	
Anterior wall	3 (18.7)
Posterior wall	4 (25.0)
Left wall	1 (6.3)
Right wall	3 (18.7)
Dome	2 (12.5)
Bottom	3 (18.8)
Spatial relationship with the bladder wall	
Protruding into the bladder cavity	11 (68.7)
Protruding into the pelvic cavity	1 (6.3)
Protruding into the bladder and pelvic cavities	4 (25.0)
Morphological characteristics	
Oval	10 (62.5)
Lobulated	4 (25.0)
Fusiform	2 (12.5)
Tumor margin	
Well-defined	14 (87.5)
Ill-defined	2 (12.5)

* Data are means ± standard deviations

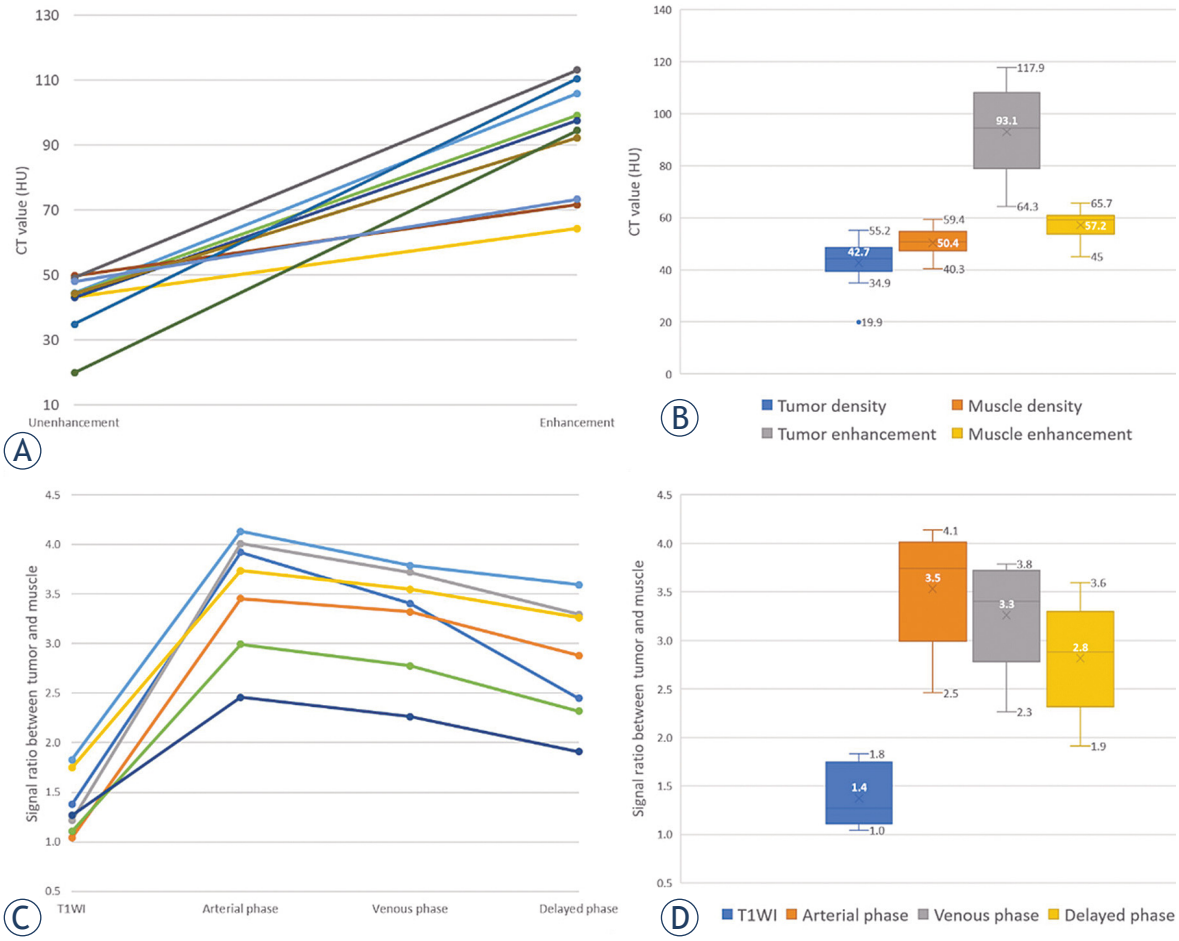

FIGURE 4. Enhancement trend charts of bladder paragangliomas on CT and MR images. **(A)** Broken line graph of enhancement trend on CT images; **(B)** Box plot of density distribution on pre- and post-contrast enhanced CT images (arterial phase); **(C)** Broken line graph of dynamic enhancement trend on MR images; **(D)** Box plot of signal distribution on unenhanced and dynamic contrast-enhanced MR images.

Results

Among the 16 patients enrolled (median age 51 years, interquartile range 40–63; 9 female), 12 patients had preoperative clinical symptoms, including six with typical symptoms related to micturition before surgery (increased blood pressure, headache, dizziness, pale complexion, chest tightness, palpitations, hyperhidrosis, abdominal pain), three had a long history of hypertension, two had haematuria and one had a progressive dysuria (tumour close to the trigone). The 24 h urinary vanillylmandelic acid (VMA) and urinary catecholamine concentrations were measured for five of the patients with typical symptoms, and only one patient had an elevated VMA concentration (429 nmol / 24 h; standard range, 59.1–266 nmol / 24 h). Twelve patients were accurately diagnosed as BPG (five of them took phenoxybenzamines for 1 to 2 weeks before surgery), and the remaining four patients were misdiagnosed preoperatively because of negative hormonal activity or atypical manifestation. Based on pathological confirmation, multiple paraganglioma was found in two cases (one with two lesions located in the bladder wall and the left adrenal gland and the other with two lesions located in the bladder wall and next to the left iliac vessels). (Table 1)

The maximum diameters of the BPGs ranged from 1.6 to 5.4 cm. The lesions were distributed in different locations of the bladder wall, and most of them grew into the bladder cavity (11/16) with broad-based attachment to the wall. The tumours mostly exhibited oval in shape (10/16) and well-defined margins (14/16) (Table 2). One of the two BPGs with ill-defined margins invaded the upper middle urethra and the anterior wall of the vagina

while the other encased the left iliac vein branch. (Figure 1–3)

On non-contrast CT images, the lesions mainly demonstrated homogeneous and soft-tissue density, with CT values ranging from 19.9 to 55.2 Hounsfield Units (HU). Intra-tumoural cystic degeneration or necrosis was rare (2/16). All lesions showed moderate to marked enhancement in the arterial phase of contrast-enhanced CT images (Table 3), with CT values of 64.3–117.9 HU, which were about 2.3 times that of the CT value on pre-contrast enhanced images (Figure 4A–B). In the two patients with multiple paragangliomas, the density and enhancement pattern of lesions in the non-bladder sites were similar to those in the bladder.

On T2WI, the lesions demonstrated homogenous hyperintensity (10/16), higher than the *gluteus maximus* and lower than the urine in the bladder, without typical "pepper and salt" sign. Due to the restricted diffusion, the lesions showed hyperintensity on DWI and hypointensity on ADC maps (mean ADC value ± standard deviation, 0.883 ± 0.126×10^{-3} mm^2/s). On T1WI, the lesions showed hyperintensity and averaged 1.4 times higher than that of the *gluteus maximus* at the same layer. Following MRI enhancement, the BPGs all had obvious enhancement in the arterial phase (an average of 2.5 times higher than the tumour signal intensity on T1WI), slightly decreased enhancement in the venous phase and the delayed phase (an average of 2.4 and 2.0 times higher than the tumour signal intensity on T1WI, respectively), exhibiting a "fast in and slow out" enhanced pattern (Table 3, Figure 4C–D). Similar to CT findings, the two patients with multiple paragangliomas showed comparable MRI findings between the bladder and non-bladder lesions.

Pathological examination revealed that the tumours were of varying sizes, nodular, with a greyish-tan cut surface and medium hardness. Microscopic examination showed polygonal or oval tumour cells that were rich in basophil granular cytoplasm and arranged in a sheet or organoid arrangement, which had abundant sinuses and capillaries. Immunohistochemical staining showed that the tumour cells were positive for chromogranin A (Figure 5).

TABLE 3. CT and MR image characteristics*

Computerized tomography (n = 13)	
Density	Moderate or slightly lower density
Enhancement characteristics	Moderate to marked enhancement
Calcification	None
Cystic degeneration or necrosis	Rare (n = 2)
Haemorrhage	None
Magnetic resonance imaging (n = 8)	
T2-weighted imaging	Slight hyperintensity
Diffusion-weighted imaging	Hyperintensity
Apparent diffusion coefficient (ADC) map	Hypointensity (ADC value, 0.883±0.126×10^{-3} mm^2/s)**
T1-weighted imaging	Slight hyperintensity
Enhancement characteristics	"Fast in and slow out" pattern
Cystic degeneration or necrosis	Rare (n = 2)
Haemorrhage	None

* The density and signal intensity of the tumours were reported with reference to those of the *gluteus maximus* in the same layer; ** data are means ± standard deviations

Discussion

BPG is a rare neuroendocrine neoplasm with potential hormonal activity derived from the medullary tissue of the bladder wall sympathetic nervous system.[7] Better surgical preparation and effective perioperative anaesthetics management is required to avoid potentially fatal consequences, such as hypertensive crisis. In this study, the clinical and imaging characteristics of 16 patients with BPG were documented and analysed.

Several typical BPG symptoms caused by catecholamine release, such as hypertension, headache, palpitations, and perspiration, were present in 83% of BPG patients.[8] Because of the special location of BPGs, the above symptoms may be caused by over distension of the bladder, micturition or defecation.[7] In this study, 75% of patients had typical symptoms, which was consistent with previous literature. Similar to other paragangliomas, BPGs can usually be diagnosed by biochemical tests, such as 24 h urine measurements of catecholamines or metabolites. However, some BPGs showed no biochemical abnormalities, as were the lesions in this study, which may be due to the small size of the tumour at diagnosis or the transient hormone-release during micturition.[2]

BPGs have the predilection age of 30–50 years with no gender difference. Primary lesions can occur in any part of the bladder wall and mainly have cavity growth with a size ranging from 1.2–5.0 cm.[9] The ages and tumour sizes of the 16 patients were compatible with the reported information. BPGs are prone to attach to the bladder wall with a broad base. This morphological characteristic was observed in all 16 lesions, which may be

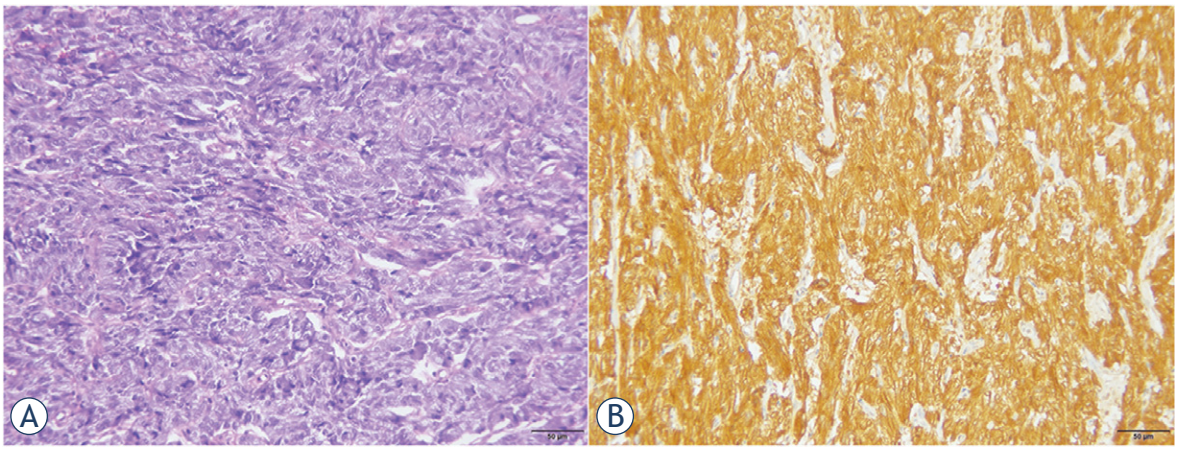

FIGURE 5. Microscopic examination of paraganglioma. **(A)** Polygonal or oval tumour cells were rich in basophil granular cytoplasm and arranged in a sheet or organoid arrangement. (Hematoxylin and eosin staining, × 400). **(B)** Immunohistochemical staining of tumours cells was positive for chromogranin A (CgA) (EnVision × 200).

pathologically based on the tendency of BPGs to infiltrate and grow along the muscularis.[10] Lu *et al.* suggested that intramural (located in the muscular layer) and subserosal (protruding from the serosa) tumours often had systemic symptoms caused by catecholamine release. Furthermore, the tumours with typical manifestations were larger than those without typical manifestations.[7] In this study, 50% and 100% of the intramural and subserosal tumours showed systemic manifestations, respectively, but the correlation between symptoms and sizes was not observed.

Imaging methods are primarily used for localization of the paraganglioma.[11] In the absence of typical clinical manifestations and negative biochemical tests, imaging can also be used as a complementary approach for qualitative diagnosis. CT has a high sensitivity (82%) in detecting extra-adrenal pheochromocytoma.[9] We demonstrated that most BPGs are typically present as a solitary lesion protruding into or out of the bladder cavity, with an oval shape, soft tissue density, well-defined margin and a broad-base attachment to the bladder wall. The tumour exhibits slightly lower density and early marked enhancement on the contrast-enhanced CT images. Contrary to the previous literature, T2WI showed that BPGs are mostly homogeneous and high-intensity, without the typical "pepper and salt" appearance.[12,13] The homogenous nature may be due to the fact that the lesion was still small when it was detected, and intratumoural degeneration has not yet occurred. Similar to bladder cancer, BPGs show marked hyperintensity on DWI and hypointensity on ADC maps due to restricted diffusion of water molecules.[14] The tumours presented slight hyperintensity on T1WI and "fast in and slow out" enhanced pattern on contrast-enhanced images, which may be distinctive MRI features of BPGs.[10,15] The potential pathological bases for the above imaging findings are that the tumour cells are large with abundant cytoplasm and the intercellular stromata are rich in blood vessels showing fissure or haemangioma-like dilatation.[16]

The malignant rate of BPGs is estimated to be 10–15%.[9] Because no reliable pathological evidence exists for early differentiation between benign and malignant tumours, direct invasion of adjacent tissues or distant metastases are considered to represent potential malignancy.[17] In this study, two lesions showed features of peripheral tissue invasion, suggesting malignancy. At present, dynamic contrast-enhanced MRI incorporating non-fat suppression T2WI with small FOV and high resolution, by means of the natural contrast between pelvic fat and urine in bladder, is the preferred imaging method for recognition of possible malignant tumours.[18] In addition to CT and MRI, functional imaging is recommended to detect multi-focal and metastatic disease, such as ^{123}I-metaiodobenzylguanidine (^{123}I-MIBG) SPECT and ^{68}Gallium-labeled somatostatin analogues (^{68}Ga-DOTA-SSA) PET/CT. Depending on specific ligands that target specific cell membrane transporters or vesicular catecholamine transport systems, this modality can provide greater diagnostic specificity.[12,19]

Due to their rarity and symptomatic variability, BPGs, especially malignant BPGs, should be differentiated from bladder carcinoma, the most

common malignant tumour of the bladder. The latter is more likely to occur in older men, related to smoking, and includes common symptoms of painless gross haematuria and progressive dysuria. Bladder carcinoma mostly shows hypointensity on T1WI compared to the appearance of muscle and no early marked enhancement. This may be the crucial difference between these two kinds of tumours. Other infrequent tumours of the bladder, such as lymphoma leiomyoma and haemangioma, cannot be ignored and they can be distinguished from BPGs by comprehensive analysis of CT and MRI characteristics.

This study has limitations. It is a retrospective series of a small study population, imaging with CT and MRI was not available in all patients, and contrast-enhanced CT contained only plain and arterial phase images. Although we attempted to objectively describe the image characteristics by calculating tumour-muscle signal ratio, due to the different scanners, inconsistent image acquisition time and subjective observation, the features observed require further validation in more cases.

In conclusion, on CT and MRI, BPGs are mostly oval-shaped, well-defined and broadly-based bladder tumours with hypoattenuation on non-contrast CT, T2 hyperintensity, slight T1 hyperintensity compared to the muscle, marked restricted diffusion on DWI and "fast in and slow out" enhanced pattern on contrast-enhanced images. Preoperative CT and MRI can be used to determine the location of the tumours, but can also assist in qualitative diagnosis, malignant risk assessment and operative proposal formulation.

Acknowledgement

We acknowledge financial support from the National Natural Science Foundations of China (Grant No. 81971580 and No. 81471641-JT); the Medical Big Data Research and Development Project supported by Chinese PLA General Hospital (Grant No. 2018MBD-023).

Reference

1. Lenders JW, Duh QY, Eisenhofer G, Gimenez-Roqueplo AP, Grebe SK, Murad MH, et al. Pheochromocytoma and paraganglioma: an endocrine society clinical practice guideline. *J Clin Endocrinol Metab* 2014; **99:** 1915-42. doi: 10.1210/jc.2014-1498

2. Beilan JA, Lawton A, Hajdenberg J, Rosser CJ. Pheochromocytoma of the urinary bladder: a systematic review of the contemporary literature. *BMC Urol* 2013; **13:** 22. doi: 10.1186/1471-2490-13-22

3. Qin J, Zhou G, Chen X. Imaging manifestations of bladder paraganglioma. *Ann Palliat Med* 2020; **9:** 346-51. doi: 10.21037/apm.2020.03.09

4. Sharma AP, Bora GS, Mavuduru RS, Panwar VK, Mittal BR, Singh SK. Management of bladder pheochromocytoma by transurethral resection. *Asian J Urol* 2019; **6:** 298-301. doi: 10.1016/j.ajur.2018.05.010

5. Tevosian SG, Ghayee HK. Pheochromocytomas and paragangliomas. *Endocrinol Metab Clin North Am* 2019; **48:** 727-50. doi: 10.1016/j.ecl.2019.08.006

6. International Agency for Research on Cancer. World Health Organization. *WHO classification of tumours of endocrine organs*. 4th edition. Lloyd RV, Osamura RY, Klöppel G, Rosai J, editors. Lyon, France: IARC; 2017. p. 78-80.

7. Lu H, Male M, Jiang K, Ye Z, Song D, Xia D. Clinical significance of functional and anatomical classifications in paraganglioma of the urinary bladder. *Urol Oncol* 2019; **37:** 354.e9-17. doi: 10.1016/j.urolonc.2019.01.027

8. Jain A, Baracco R, Kapur G. Pheochromocytoma and paraganglioma-an update on diagnosis, evaluation, and management. *Pediatr Nephrol* 2020; **35:** 581-94. doi: 10.1007/s00467-018-4181-2

9. Henderson SJ, Kearns PJ, Tong CM, Reddy M, Khurgin J, Bickell M, et al. Patients with urinary bladder paragangliomas: a compiled case series from a literature review for clinical management. *Urology* 2015; **85:** e25-9. doi: 10.1016/j.urology.2014.11.006

10. Liu F, Xiao H, Wang H, Fang Z, Yu Y, Li Y, et al. [The imaging analysis and diagnosis of the paraganglioma of the urinary bladder]. [Chinese]. *Oncoradiology* 2020; **29:** 181-6. doi: 10.19732/j.cnki.2096-6210.2020.02.018

11. Sbardella E, Grossman AB. Pheochromocytoma: an approach to diagnosis. *Best Pract Res Clin Endocrinol Metab* 2020; **34:** 101346. doi: 10.1016/j.beem.2019.101346

12. Aygun N, Uludag M. Pheochromocytoma and paraganglioma: from clinical findings to diagnosis. *Sisli Etfal Hastan Tip Bul* 2020; **54:** 271-80. doi: 10.14744/SEMB.2020.14826

13. Liang JP, Li HG, Gao LK, Yin L, Yin L, Zhang JW. Bladder paraganglioma: Clinicopathology and magnetic resonance imaging study of five patients. *Urol J* 2016; **13:** 2605-11. doi: 10.22037/uj.v13i2.3140

14. Al Johi RS, Seifeldein GS, Moeen AM, Aboulhagag NA, Moussa EM, Hameed DA, et al. Diffusion weighted magnetic resonance imaging in bladder cancer, is it time to replace biopsy? *Cent European J Urol* 2018; **71:** 31-7. doi: 10.5173/ceju.2017.1427

15. Wang H, Ye H, Guo A, Wei Z, Zhang X, Zhong Y, et al. Bladder paraganglioma in adults: MR appearance in four patients. *Eur J Radiol* 2011; **80:** e217-20. doi: 10.1016/j.ejrad.2010.09.020

16. Fan DG, Wu CL, Huang HJ, Wu L, Lin SY. [Paraganglioma of urinary bladder: a clinicopathological features analysis of 23 cases]. [Chinese]. *Zhonghua Bing Li Xue Za Zhi* 2020; **49:** 311-6. doi: 10.3760/cma.j.cn112151-20190928-00535

17. Quist EE, Javadzadeh BM, Johannesen E, Johansson SL, Lele SM, Kozel JA. Malignant paraganglioma of the bladder: a case report and review of the literature. *Pathol Res Pract* 2015; **211:** 183-88. doi: 10.1016/j.prp.2014.10.009

18. Raza SA, Jhaveri KS. MR imaging of urinary bladder carcinoma and beyond. *Radiol Clin North Am* 2012; **50:** 1085-110. doi: 10.1016/j.rcl.2012.08.011

19. Lenders JWM, Eisenhofer G. Update on modern management of pheochromocytoma and paraganglioma. *Endocrinol Metab (Seoul)* 2017; **32:** 152-61. doi: 10.3803/EnM.2017.32.2.152